Key events during the transition from rapid growth to quiescence in budding yeast require posttranscriptional regulators

Lihong Li, Shawna Miles, Zephan Melville*, Amalthiya Prasad, Graham Bradley, and Linda L. Breeden
Basic Science Division, Fred Hutchinson Cancer Research Center, Seattle, WA 98109

ABSTRACT **Yeast that naturally exhaust the glucose from their environment differentiate into three distinct cell types distinguishable by flow cytometry. Among these is a quiescent (Q) population, which is so named because of its uniform but readily reversed G1 arrest, its fortified cell walls, heat tolerance, and longevity. Daughter cells predominate in Q-cell populations and are the longest lived. The events that differentiate Q cells from nonquiescent (nonQ) cells are initiated within hours of the diauxic shift, when cells have scavenged all the glucose from the media. These include highly asymmetric cell divisions, which give rise to very small daughter cells. These daughters modify their cell walls by Sed1- and Ecm33-dependent and dithiothreitol-sensitive mechanisms that enhance Q-cell thermotolerance. Ssd1 speeds Q-cell wall assembly and enables mother cells to enter this state. Ssd1 and the related mRNA-binding protein Mpt5 play critical overlapping roles in Q-cell formation and longevity. These proteins deliver mRNAs to P-bodies, and at least one P-body component, Lsm1, also plays a unique role in Q-cell longevity. Cells lacking Lsm1 and Ssd1 or Mpt5 lose viability under these conditions and fail to enter the quiescent state. We conclude that posttranscriptional regulation of mRNAs plays a crucial role in the transition in and out of quiescence.**

Monitoring Editor
Mark J. Solomon
Yale University

Received: May 7, 2013
Revised: Sep 25, 2013
Accepted: Sep 26, 2013

INTRODUCTION

A unified view of the mitotic cell cycle has emerged from decades of research. However, we know surprisingly little about how cells achieve a prolonged yet reversible nondividing state. The need to control proliferation is just as important and just as conserved as proliferation itself. Cells that spend the bulk of their time in a nondividing state but are capable of cell cycle reentry must evolve mechanisms that enable them to conserve their resources, survive environmental changes, and maintain genetic stability. This is commonly referred to as the quiescent state. Multicellular organisms depend on the persistence and genetic stability of quiescent stem cells for their controlled growth, development, and tissue renewal (Tothova and Gilliland, 2007; Sang *et al.*, 2008). Stem cells are maintained in this protective resting state and divide only when stimulated to do so. Unscheduled exit from the quiescent state or defects preventing entry into the quiescence state result in uncontrolled proliferation, and the pathways controlling these decisions are defective in most if not all human tumors (Hanahan and Weinberg, 2000, 2011; Pinkston *et al.*, 2006).

Budding yeast and other microorganisms capable of rapid cell division spend the vast majority of their time in a nondividing state. Their success as species depends on their ability to enter a protective, quiescent state and readily reverse that state when conditions improve. Achieving a quiescent state involves down-regulation of the machinery of growth and proliferation, and these pathways are fundamentally conserved. As such, the strategies used by budding yeast for arresting and maintaining this quiescent state may also be conserved. With this in mind, we began an investigation of the pathway to quiescence in budding yeast.

Quiescence in budding yeast is triggered by a waning nutrient supply. However, work over many decades has shown that these cells are not starved. Well before nutrients are exhausted, these

This article was published online ahead of print in MBoC in Press (http://www.molbiolcell.org/cgi/doi/10.1091/mbc.E13-05-0241) on October 2, 2013.

*Present address: Center for Biomolecular Therapeutics and Department of Biochemistry and Molecular Biology, University of Maryland School of Medicine, Baltimore, MD 21201.

Address correspondence to: Linda Breeden (lbreeden@fhcrc.org).

Abbreviations used: DS, diauxic shift; FACS, fluorescence-activated cell sorting; nonQ, nonquiescent; Q, quiescent.

cells redirect their resources and metabolism, which enables them to conserve and stockpile critical provisions, including glucose, phosphate, and fatty acids (Lillie and Pringle, 1980; Francois and Parrou, 2001; De Virgilio, 2012). Glucose is stored in the form of glycogen and trehalose. These storage carbohydrates provide a ready energy source when division resumes (Sillje *et al.*, 1999). Trehalose also stabilizes and protects proteins and membranes (Elbein *et al.*, 2003) from dehydration (Gadd *et al.*, 1987), heat shock (De Virgilio *et al.*, 1994; Hottiger *et al.*, 1994; Ribeiro *et al.*, 1997), and oxidative damage (Benaroudj *et al.*, 2001). More recently, trehalose accumulation was shown to be required for the density shift that enables a subset of cells in a stationary phase culture to be purified (Johnston *et al.*, 1977; Allen *et al.*, 2006; Shi *et al.*, 2010). These cells are uniformly arrested in G1 and display high thermotolerance (Allen *et al.*, 2006) and longevity (Li *et al.*, 2009). Because of these properties, they have been referred to as quiescent (Q) cells. It has been suggested that trehalose accumulation could be responsible for all these Q-cell properties. However, we show that an *ssd1-d* mutant contains wild-type levels of trehalose and glycogen but reduces the yield, thermotolerance, and longevity of Q cells. Hence we conclude that trehalose accumulation may be necessary but it is not sufficient to confer these Q-cell properties.

Under the conditions we employ, the transition to the quiescent state is triggered before the diauxic shift (DS) when cells have taken up all the available glucose from their environment. G1 arrest is initiated before the DS and is maintained by the transcriptional repression of the *CLN3* cyclin by Xbp1 (Miles *et al.*, 2013). This is followed by an unusually asymmetric cell division, which gives rise to a large population of very small daughter cells. Shortly thereafter, we detect changes by flow cytometry that are the result of elaborate fortifications of their cell walls. These events differentiate the Q-cell lineage from their nonquiescent (nonQ) siblings and enable us to track their progress, purify, and characterize them.

When the glucose level drops to 0.6% there is a rapid drop in global translation initiation (Castelli *et al.*, 2011). Glucose depletion causes an equally rapid accumulation of mRNA in processing bodies (P-bodies; Teixeira *et al.*, 2005), where these mRNAs are either degraded or sequestered. mRNAs in the P-bodies that accumulate during stationary phase can return to translation (Brengues *et al.*, 2005) due to the recruitment of translation initiation factors (Brengues and Parker, 2007; Hoyle *et al.*, 2007) and two highly conserved proteins (Igo1 and 2) that inhibit the degradation of specific mRNAs critical for the transition to quiescence (Talarek *et al.*, 2010). In this way, the cell rapidly shifts the spectrum of translatable mRNAs from a proliferation- to a quiescence-specific subset.

We previously showed that Ssd1 increases the yield and longevity of Q cells (Li *et al.*, 2009). Ssd1 is an mRNA-binding and P-body associated protein (Hogan *et al.*, 2008; Jansen *et al.*, 2009; Kurischko *et al.*, 2011), which has shared roles with another mRNA-binding protein, Mpt5, in many processes, including replicative life span and cell wall integrity (Kaeberlein and Guarente, 2002). Here we show that Ssd1 accelerates Q-cell–specific cell wall fortifications. Either Ssd1 or Mpt5 and at least one Ssd1-bound mRNA encoding the cell wall protein Ecm33 must be active to build these cell walls. Both Ssd1 and Mpt5 deliver mRNAs to P-bodies (Parker, 2012), and loss of the P-body component Lsm1 compromises Q-cell longevity. Cells lacking Lsm1 and either Ssd1 or Mpt5 fail to produce Q cells. These findings highlight the importance of post-transcriptional mRNA regulation in the transition from rapid growth to quiescence and identify Ssd1 and Mpt5 as key players in this process.

RESULTS

Yeast cells spend most of their time in a nondividing state. To survive these long intervals, they must undergo a stable but reversible cell cycle arrest. They must maintain basic functions and protect themselves from environmental insults without exhausting their limited resources. To investigate this process, we built a prototrophic derivative of the laboratory strain W303 (*ssd1-d*) and followed its growth from logarithmic (log) to stationary phase as they naturally exhaust the glucose from rich medium. Under these conditions, cells undergo carbon limitation and cease dividing within 2 d (Figure 1A). They exhaust the glucose from the media between 12 and 14 h, at an optical density (OD_{600}) of ~7. After this point, referred to as the DS, the cells shift to respiration. Glucose storage in the form of glycogen begins just before the DS (Figure 1B), but a massive accumulation of glycogen and the disaccharide trehalose occurs long after all the glucose has been scavenged from the media. At 48 h, the amount of stored glucose is >1000-fold higher than it is in logarithmically growing cells.

This pattern of growth and carbohydrate accumulation parallels that shown three decades ago for a prototrophic strain in response to glucose, sulfur, nitrogen, and phosphate depletion (Lillie and Pringle, 1980). It has since been shown that these stored carbohydrates are correlated with and required for a density shift that facilitates the purification of a population of cells that are in a uniform, quiescent state (Allen *et al.*, 2006; Shi *et al.*, 2010). These Q cells sediment to the bottom of a Percoll gradient, whereas the nonQ cells remain at the top. In W303 *ssd1-d*, the density shift occurs between 24 and 48 h and correlates with a threefold increase in trehalose (Figure 1B). Density is maintained by about half the cells for at least 7 d (168 h). The dense cells purified after 7 d are quiescent, based on their very long life span (Li *et al.*, 2009; Figure 1D.) These purified Q cells, in water, survive three times longer than the cells in a stationary-phase culture (Figure 1D.) Even when incubated at high cell densities (OD_{600} = 10) for 6 wk in water, Q cells remain 80% viable and do not acidify their environment (unpublished data). This is unlike stationary-phase cultures, which acidify unbuffered medium within 4 d and lose viability much more rapidly (Burtner *et al.*, 2009).

Quiescence is triggered by a diminishing supply of carbon

We infer that glucose storage is an important aspect of attaining a quiescent state because acute glucose withdrawal precludes both glucose storage and long-term survival. Figure 1D compares the viability of W303 *ssd1-d* prototrophs allowed to grow from log to stationary phase and naturally exhaust their glucose (SP) to those transferred from rich glucose media to the same media lacking glucose (glu–). These glucose-deprived cells die rapidly. They do not accumulate carbohydrate, nor do they arrest in G1 (Figure 1E.) Cells that are shifted to limiting (0.8%) glucose media for 2.5 h before glucose withdrawal have an intermediate survival (Figure 1D, lim glu). We conclude that detecting and responding to a diminishing supply of glucose (or other essential nutrients) is an important step in achieving the quiescent state. Cells that are abruptly deprived of glucose are unable to make this transition.

Thermotolerance is a property of quiescent cells

It has been argued that heat tolerance is not a consequence of entering a quiescent state because it is a general property of slowly growing cells (Elliott and Futcher, 1993; Lu *et al.*, 2009; Klosinska *et al.*, 2011). Rapidly growing cells are acutely sensitive to heat, and their thermotolerance increases by many orders of magnitude as their proliferation rate is slowed by carbon source changes (Elliott and Futcher, 1993) or glucose limitation (Lu *et al.*, 2009). This has led

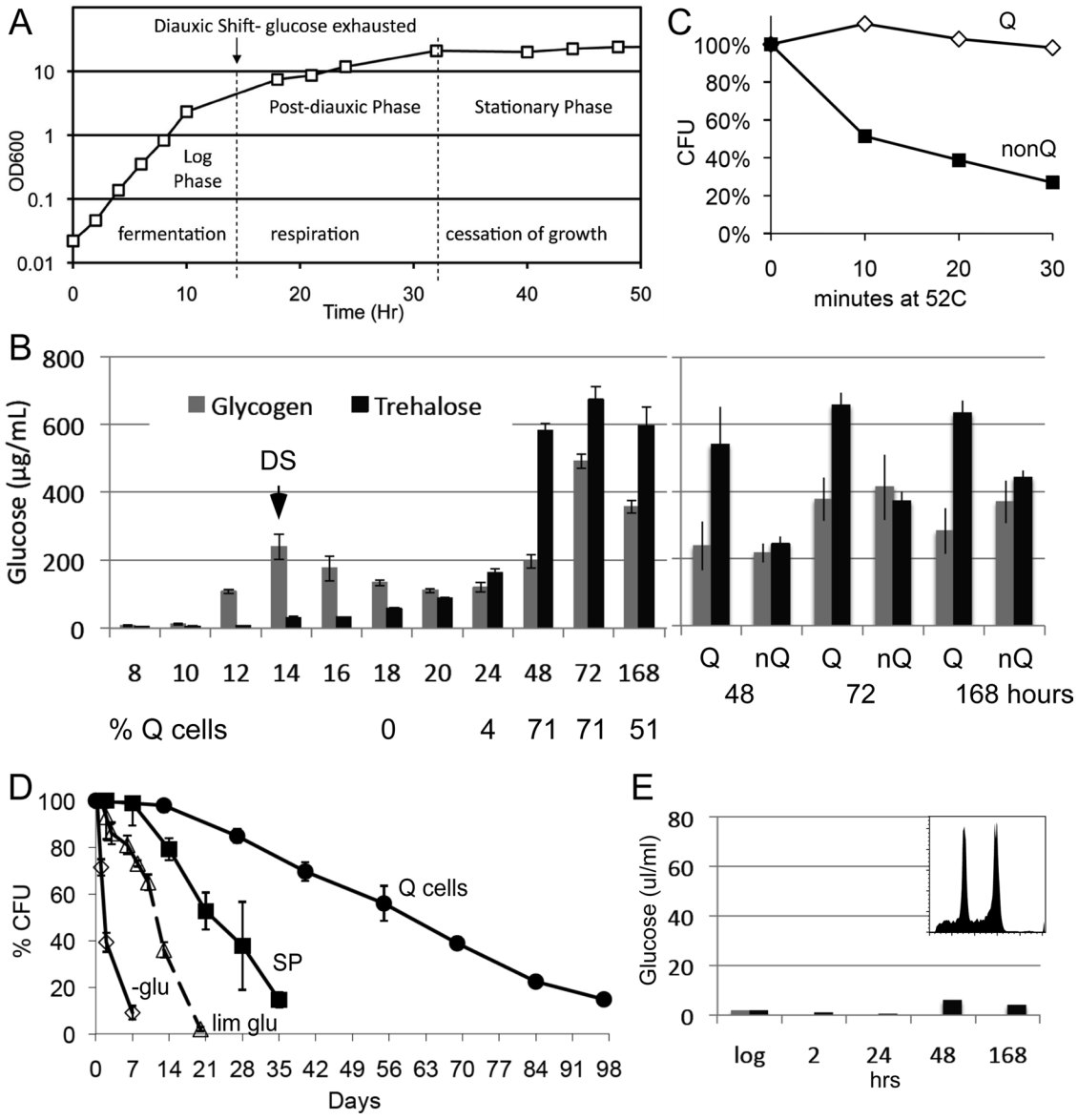

FIGURE 1: Growth of prototrophic W303 *ssd1-d* (BY6500) in rich medium from log to stationary phase produces quiescent cells. (A) Optical density of cells as a function of time after inoculation into YEPD medium. DS was defined as the time point at which glucose was no longer detectable in the medium and is marked. (B) Glucose equivalents in trehalose and glycogen from 8 h (log phase) to 168 h (stationary phase [SP]) and then in Q and nonQ cells purified after 48, 72, or 168 h. Bottom, percentage of cells fractionating as Q cells at the hours indicated. (C) Thermotolerance of purified Q and nonQ cells upon shifting to 52°C assayed as colony-forming units (CFU). (D) Survival curve for cells grown in YEP 2% glucose and then transferred to YEP 0% glucose (–glu), cells grown to SP, purified Q cells resuspended in water (Q cells) or grown in YEP 2% glucose, transferred to YEP with 0.8% glucose for 2.5 h, then transferred to YEP with 0% glucose (lim glu). (E) Glycogen and trehalose accumulation in log-phase cells grown in YEP 2% glucose and then transferred to YEP 0% glucose for the hours indicated. Inset, FACS profile of DNA from cells 168 h after glucose withdrawal.

to the suggestion that thermotolerance and other properties associated with nondividing cells (Brauer *et al.*, 2008) are due not to their transition into a discrete quiescent state but instead to the fact that they have stopped growing. If thermotolerance was simply a property of slowly dividing or nondividing cells, we would expect similar survival curves for both Q and nonQ cells (Figure 1C). These Q and nonQ cells are genetically identical and were collected by density gradient sedimentation from the same stationary-phase culture. They were stored and tested for thermotolerance in water. Neither population is dividing, but the Q cells are at least fivefold more thermotolerant than the nonQ cells. Essentially all the Q cells can reenter the cell cycle and form colonies after a 30-min heat treatment, whereas only 20% of the nonQ cells retain colony-forming ability. Clearly, there is heterogeneity in the thermotolerance of nondividing cells, and Q cells are significantly more thermotolerant than their nonQ siblings. It is also worth noting that nonQ cells have roughly equivalent levels of glycogen and only 30% less trehalose (Figure 1B). It seems unlikely that this small difference could be solely responsible for the fractionation properties or the difference in thermotolerance between the Q and nonQ populations.

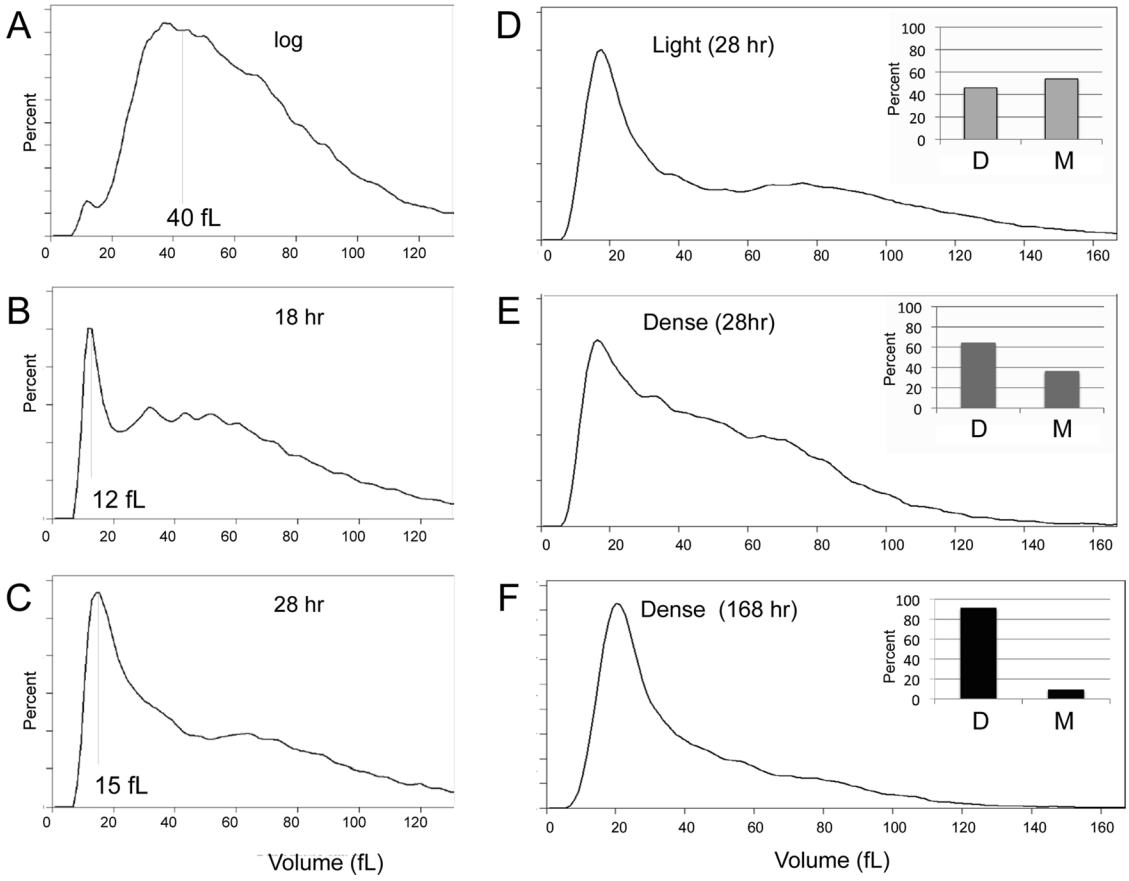

FIGURE 2: Q-cell differentiation involves asymmetric cell divisions. Size distribution of prototrophic W303 *ssd1-d* cells (A) during log phase and (B) 4 h and (C) 14 h after the DS. (D) light and (E) dense fractions after density gradient purification of cells in C. (F) Dense fraction after purification of Q cells from 7-d stationary-phase culture. Insets, mother-to-daughter ratio in the population after two gradient purifications, assayed by bud scar staining with Calcofluor.

Postdiauxic cells undergo highly asymmetric cell divisions

To characterize the events that take place during the differentiation of Q cells, we monitored cell size as cells transit from the logarithmic phase of growth to the stationary phase. During log phase, cell size is heterogeneous (Figure 2A), and the modal cell volume is ~40 fl. However, 4 h after the DS there is a dramatic change in size distribution. About 20% of cells in this population are only 12 fl in total volume (Figure 2B). These small cells continue to accumulate and become the predominant cell type in the culture 14 h post-DS (Figure 2C). Many investigators have observed the asymmetric cell divisions that give rise to small cells under poor growth conditions (Johnston *et al.*, 1977, 1979; Lord and Wheals, 1980). Our data provide a quantitative measure of extent, synchronicity, and timing of this asymmetric cell division as cells respond to glucose limitation and transit from log to stationary phase.

To establish the relationship between the density shift and the asymmetric cell division, we purified the dense population from a 28-h-old culture. At this early stage, when 30% of the cells purify in the Q fraction, there is only a slight enrichment for daughter cells (Figure 2, D and E). This is in contrast to the Q cells purified from a 7-d-old stationary phase culture, which have a modal cell volume of ~22 fl and are 86% daughters and 13% young mothers (Figure 2F). These studies show that initially both mothers and daughters can shift to the higher cell density. However, daughters and young mothers are better able to maintain this density. In addition, it is clear that small daughters are not born dense; they must acquire this characteristic.

A partial explanation for this comes from the asymmetry of mitochondrial function in mothers and daughters, which was observed by Lai *et al.* (2002) and linked to longevity. Because carbohydrate accumulation is required for the density shift of Q cells, it follows that these primarily daughter cells shift to respiration, whereas the nonQ cells continue to exhaust their glucose supply through glycolysis. Cells in the Q fraction contain higher levels of many mitochondrial proteins and consume six times more oxygen than the nonQ cells (Davidson *et al.*, 2011). We used green fluorescent protein (GFP)–tagged Abf2, which coats mitochondrial DNA (Caron *et al.*, 1979), to look at its organization in the Q and nonQ fractions. By flow cytometry (Figure 3A), Q cells show a sharp peak of high Abf2-GFP fluorescence. The nonQ cells show an overlapping but very broad peak, indicating significant reduction and heterogeneity in the fluorescence signal. The difference is even more striking in fluorescent images (Figure 3B), which show strong punctate localization of Abf2 in every Q cell. The nonQ cells, in contrast, show much more diffuse and heterogeneous Abf2-GFP signal. This highly uniform mitochondrial DNA staining in Q cells marks another striking asymmetry between the Q and nonQ populations.

Aggregates of actin accumulate in stationary phase cells as they exhaust their glucose (Sagot *et al.*, 2006). It has been suggested that these aggregates could be a defining property or marker of

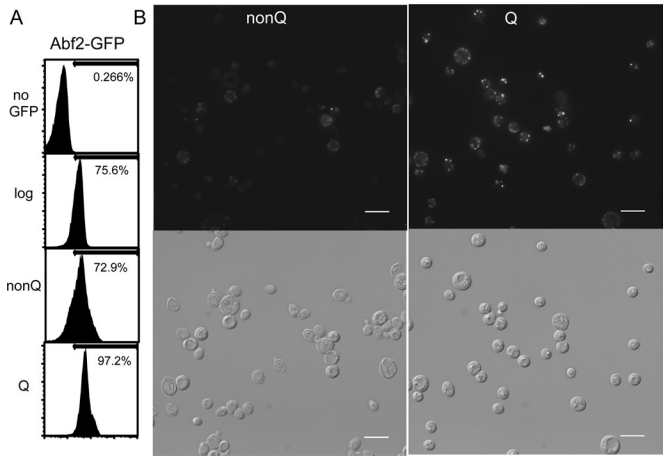

FIGURE 3: Mitochondrial DNA (mtDNA) inheritance asymmetry in nonQ (nQ) and Q cells. (A) Fluorescence from mtDNA binding protein Abf2 fused to GFP was assayed in GFP-negative cells or Abf2-GFP cells (BY7078) in log phase and purified nonQ and Q cells. (B) Abf2-GFP localized in nonQ and Q cells. Scale bar, 10 μm.

quiescence (Laporte *et al.*, 2011). We used phalloidin to stain actin aggregates and found them to be indistinguishable in the Q and nonQ populations (Supplemental Figure S1). Hence actin aggregation is not correlated with quiescence under these conditions.

Transition to quiescence is correlated with discrete and reversible changes in the cell wall that can be detected by flow cytometry

After 18 h of growth, when the very small daughters are prevalent and most of the cells are in G1, another striking change in pre-Q cells becomes evident. A new peak of DNA can be seen in the flow cytometry profile (Figure 4A) that is indicative of lower fluorescence intensity. This novel DNA peak gradually becomes more prominent until, at 28 h, about half the DNA is shifted. It is this DNA profile that predominates in the purified Q cells (Figure 4A, bottom). On refeeding, there is an equally discrete shift of the Q DNA peak back to the state observed with log-phase cells in G1 (Figure 4B).

Cells entering quiescence also display unique light scattering properties. Figure 4C shows forward versus side light scattering of a culture in the log phase of growth. Despite the fact that they are in all phases of the cell cycle (Figure 4D), they form a single tight cluster based on light scattering. In dramatic contrast, a culture that has grown for 24 h and is largely in G1 scatters much more light and splits into three discrete populations (Figure 4E). We sorted these populations using the gates indicated as R1, R2, and R3. The DNA fluorescence, differential interference contrast (DIC) images, and Calcofluor staining of these populations are shown in Figure 4F. The R1 cells scatter the least amount of light and represent 20% of the total population. They are homogeneous, unbudded, and very small. They show a bright but uniform staining with Calcofluor, with no bud scars, indicating that they are very small daughter cells. They are all in G1, and their DNA is slightly reduced in fluorescence intensity compared with R2 cells. The R2 cells represent almost half the population at this time point. R2 includes most of the mother cells with prominent bud scars and all the cells that failed to G1 arrest. Their DNA fluorescence intensities are comparable to those of log-phase cells. R3 is also primarily composed of daughter cells. They are clearly larger than the R1 cells, and there are some young mothers within this population. It is the R3 cells that contain the DNA fluorescence profile of purified Q cells (compare Figure 4, A, bottom, with F, bottom left, and I, top).

The DNA fluorescence and the light scattering properties of the cells present at 24 h indicate that this population has differentiated into at least three distinct cell types. One likely contributor to these changes is the cell wall. Cells in stationary phase are known to have stronger cell walls than growing cells, and one of the major wall components during stationary phase is Sed1 (Shimoi *et al.*, 1998). Sed1 is induced at the DS and enables stationary-phase cell walls to resist enzymatic digestion. We repeated the cytometry with a *sed1* mutant grown for 24 h and found that both the reduced DNA fluorescence and the heterogeneous light scattering are eliminated by loss of this cell wall protein (Figure 4G).

As a further test, we treated a 24-h-old culture with dithiothreitol (DTT). This reducing agent strips the cell wall of mannoproteins that are linked to it by disulfide bridges (Salazar and Asenjo, 2007). A 15-min treatment with this reducing agent was sufficient to increase DNA fluorescence intensity back to that of log-phase cells and dramatically reduce light scattering (Figure 4H.) The simple interpretation of these results is that Sed1 and other disulfide-linked proteins are required for the additions to the cell wall that resist dye penetration and cause the striking and heterogeneous light scattering properties of cells that arise as they transit from growth to stationary phase.

These cell wall changes are initiated shortly after the DS, when *SED1* expression is induced. In W303 *ssd1-d* there must be some asymmetry to this process because the daughter cells destined to become Q cells develop different cell wall properties than their nonQ mothers. Hence these cell wall changes, which can be quantified by flow cytometry, provide a convenient marker of developing Q cells that is independent of their shift in density. If these cell wall changes are an important characteristic of Q cells, we expected them to play a protective role. To test this, we treated Q cells with DTT and then assayed their thermotolerance. DTT treatment reduced light scattering and promoted dye penetration of Q cells (Figure 4I). It also made Q cells much more thermosensitive than untreated Q cells (Figure 4J). Hence thermotolerance is not strictly dependent on trehalose accumulation. These cell wall modifications also contribute by forming a protective barrier to environmental changes.

Ssd1 promotes the quiescence and longevity of mother cells

We previously reported that prototrophic W303 carrying the *SSD1* allele produces nearly twice as many Q cells as the isogenic strain carrying the truncated *ssd1-d* allele (Li *et al.*, 2009). This is especially pronounced under long-term culture conditions (Figure 5A). Moreover, these purified Q cells survive in a nondividing state twice as long, and it is the ability to reenter the cell cycle, rather than cell viability, that is compromised by the loss of Ssd1 activity (Li *et al.*, 2009). *SSD1* Q cells are also more thermotolerant (Figure 5B), and upon refeeding, they recover and reenter the cell cycle more rapidly than W303 *ssd1-d* (see later discussion of Figure 7C). It has been suggested that differences in yield, longevity, thermotolerance, and recovery of Q cells could all be due to the high levels of glycogen and trehalose stored by these cells (Shi *et al.*, 2010). However, *SSD1* and *ssd1-d* stationary-phase cultures and purified Q cells accumulate equivalent levels of stored carbohydrate (Figure 5C). Clearly, the levels of these compounds cannot be solely responsible for the increased yield, thermotolerance, longevity, or recovery of *SSD1* Q cells. Carbohydrate accumulation may be necessary, but it is not sufficient to confer these quiescent phenotypes.

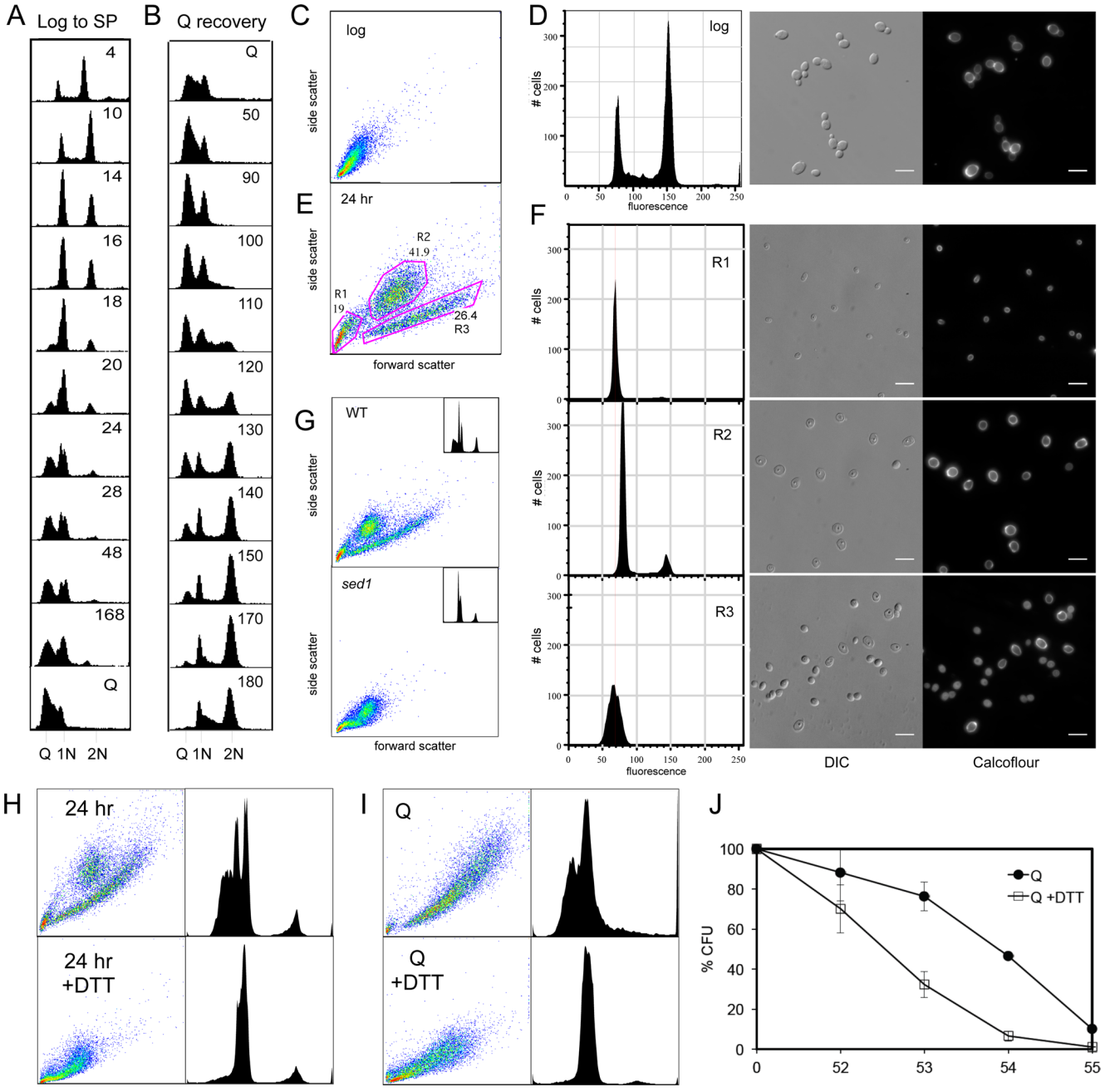

FIGURE 4: Stationary-phase cultures contain three distinct cell types. (A) FACS profile of DNA from W303 *ssd1-d* prototrophs (BY6500) as they grow from log to stationary phase. Bottom, DNA from Q cells purified from the 168-h culture. (B) FACS profile of DNA as purified Q cells reenter the cell cycle after resuspension in fresh YEPD media. Cells were collected every 15 min as indicated. (C) Scatter plot of forward and side light scattering of log-phase cells. (D) FACS profile of DNA, DIC, and fluorescence images of log-phase cells stained with Calcofluor. (E) Light scattering of cells grown for 24 h to the post-DS phase of growth, showing three distinct cell types in gates R1, R2, and R3 and the percentage of each. (F) FACS profile of DNA, DIC, and Calcofluor-stained images of cells sorted with the gates in E. Scale bar, i10 µm. Light scattering and DNA fluorescence profile (inset) for (G) *sed1* mutant (BY7149) grown for 24 h and (H) wild-type cells grown for 24 h and then treated with DTT. (I) Purified Q cells with and without DTT treatment. (J) DTT-treated and untreated Q cells incubated at 52–55°C for 10 min and plated.

The fact that W303 *SSD1* produces almost 80% Q cells indicates that many mother cells enter quiescence in this genetic background. Not only do they develop the density of their daughters, but their longevity in the nondividing state is also extended. We followed the longevity of mother and daughter Q cells in this population by costaining with Calcofluor and propidium iodide. Calcofluor stains bud scars, which identifies mothers, and propidium iodide stains dead cells (Figure 5D). After 2 wk, viability is 97%, and the fraction of mother and daughter cells is comparable (Figure 5, E and F). Even after 10 wk, mothers are surviving, but the youngest mothers with only one bud scar predominate. This trend continues for 18 wk, when only 21% of the Q cells are viable. At this time point, 80% of

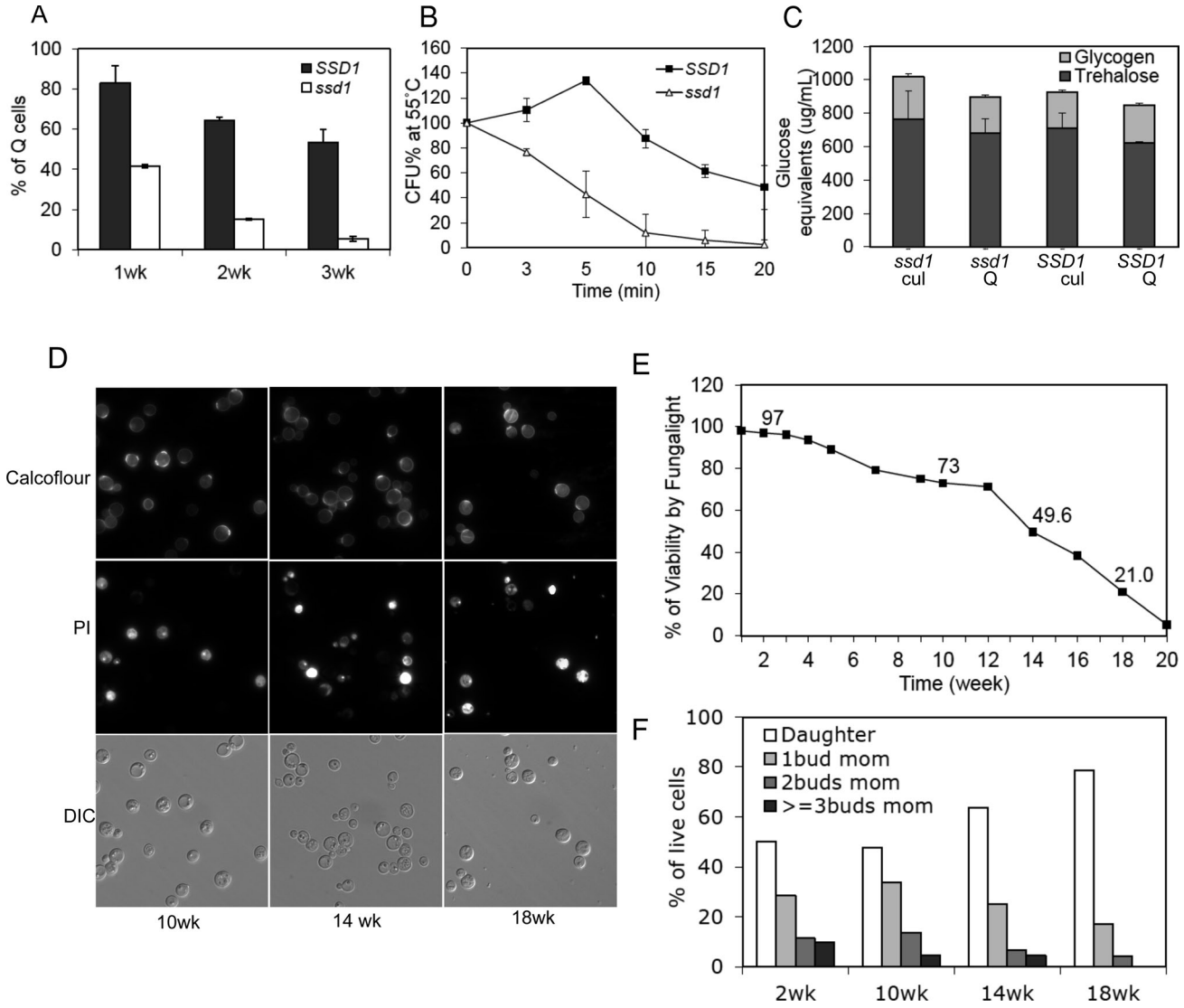

FIGURE 5: Quiescent daughters outlive quiescent mothers. (A) W303 *SSD1* and *ssd1-d* cells assayed for Q-cell yield at 1, 2, or 3 wk after inoculation into YEPD medium. (B) Thermotolerance of 1-wk-old Q cells as measured by colony-forming units (CFU) after 0–20 min at 55°C. (C) Trehalose and glycogen accumulation in stationary-phase cultures and Q cells. (D) *SSD1* Q cells stained for bud scars (Calcofluor), dead cells (propidium iodide [PI]), and DIC after 10, 14, and 18 wk of suspension in water. (E) Q cells in D monitored for viability and (F) scored for live daughter and mother cells.

the viable cells are daughters and 15% are mothers that have undergone a single division. We conclude that the asymmetry at division that promotes quiescence of daughter cells still exists in W303 *SSD1*, but *SSD1* enables mother cells to adopt a similar, if somewhat compromised, quiescent state.

SSD1 accelerates cell wall modification during stationary phase

The high yield and longevity of *SSD1* Q cells and the importance of cell wall modification for Q-cell protection suggest that Ssd1 may play a role in Q-cell wall formation. Ssd1 is an mRNA-binding protein whose target mRNAs are enriched for transcripts encoding cell wall components and proteins that localize to the bud (Hogan *et al.*, 2008). Ssd1 also binds several mRNAs that are transcribed only in daughter cells and whose products promote the separation of mother from daughter (Hogan *et al.*, 2008; Jansen *et al.*, 2009). Ssd1 associates with P-bodies and stress granules during glucose depletion, heat shock, and salt stress (Jansen *et al.*, 2009; Kurischko *et al.*, 2011). These are sites to which mRNAs are recruited to be degraded or stored and translationally repressed (Balagopal and Parker, 2009). Evidence suggests that Ssd1 delivers mRNAs to these sites and represses their translation until they are needed for cell wall growth and cell separation (Jansen *et al.*, 2009; Kurischko *et al.*, 2011). Ssd1 also transiently associates with the bud cortex and promotes delivery of *SRL1* mRNA to the bud (Kurischko *et al.*, 2011). *SRL1* is one of many mRNAs encoding cell wall proteins that are bound by Ssd1 (Hogan *et al.*, 2008).

As described earlier, Q-cell walls have unique light scattering properties and increased resistance to dye penetration. To see whether Ssd1 plays a role in the elaboration of Q-cell walls, we used flow cytometry to follow *SSD1* and *ssd1-d* cells as they shifted from logarithmic to stationary phase of growth. Light scattering is largely unaffected by Ssd1. However, the peak of reduced DNA fluorescence appears 6 h earlier in the *SSD1* strain, and nearly all the cells attained this characteristic after 40 h (Figure 6A). This shift occurs, but much more slowly, in *ssd1-d* cells. The fact that these two cell

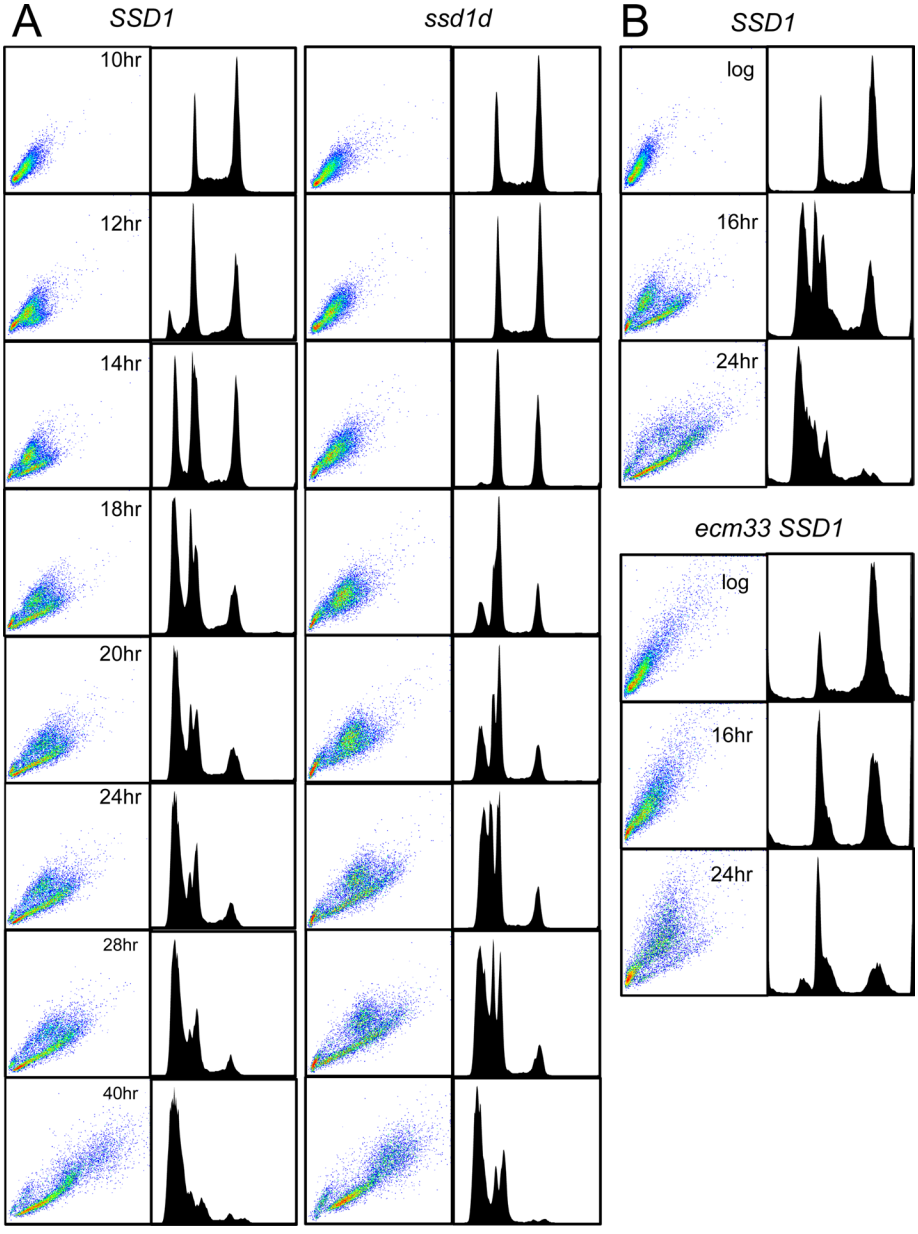

FIGURE 6: *SSD1* promotes cell wall modification. (A) Light scattering (left) and DNA fluorescence plots (right) of W303 *SSD1* and *ssd1-d* cells as they grow from log to stationary phase. (B) The same plots for W303 *SSD1* and W303 *SSD1 ecm33* during log phase or after 16 and 24 h of growth.

wall phenotypes can be genetically separated indicates that they are mechanistically distinct. We conclude that *SSD1* facilitates the barrier to dye penetration but does not influence the light scattering properties of stationary-phase cells. To see whether mRNAs bound by Ssd1 are also important, we assayed cells with and without Ecm33. Figure 6B shows that this protein, whose mRNA is bound by Ssd1 (Hogan *et al.*, 2008), is also required for resisting dye uptake but not for light scattering.

mRNA-binding proteins Ssd1 and Mpt5 have overlapping roles in quiescence

If Ssd1 mRNA binding promotes Q-cell formation, we wondered whether Mpt5, a second mRNA-binding protein with partially overlapping functions, might also play a role. Consistent with this, we found that *mpt5* reduces Q-cell yield by about half in *SSD1* cells (Figure 7A) and shows a modest drop in carbohydrate accumulation (Figure 7B). The Q cells that are formed reenter the cell cycle more slowly than either *SSD1* or *ssd1-d* cells (Figure 7C) and have shortened life span (Figure 7D). Hence Mpt5 makes a unique contribution to Q-cell yield, recovery, and longevity. In an *ssd1-d* background, Mpt5 is absolutely required for Q-cell formation and carbohydrate accumulation. To see whether the cell wall is affected by *mpt5*, we grew mutant and wild-type cells to the postdiauxic phase (24 h), split the culture, and treated one-half with DTT. Figure 8A shows the resulting light scattering and DNA fluorescence profiles. The *mpt5* single mutant has no effect on either, but the *mpt5 ssd1-d* double mutant is aberrant by both assays. These cells display more light scattering, only a portion of which is DTT sensitive, and there is no sign of reduced DNA fluorescence. We conclude that Ssd1 and Mpt5 have overlapping functions required for carbohydrate accumulation, cell wall modification, and Q-cell formation.

We also measured a set of growth and viability parameters during log and stationary phases to see whether the *mpt5* defects are specific to stationary phase. We found that with or without *SSD1*, *mpt5* mutants grow with normal doubling times and spend the same amount of time in G1 as *MPT5* cells during logarithmic growth (Figure 8C). The viability and colony-forming ability of the *mpt5ssd1-d* double mutant is somewhat compromised, being ~35% lower than *ssd1-d* alone during log phase. During stationary phase, the *mpt5* single mutant also attains high cell density and suffers only a modest drop in viability (Figure 8D). However, the *mpt5ssd1-d* double-mutant culture stops growth at half the cell density of *ssd1-d* and suffers a threefold and fourfold loss of viability and colony formation, respectively, after 7 d of growth. Figure 8B shows the DNA fluorescence of these 7-d cultures. Fragmented DNA from dead cells accumulates on the left edge of these profiles. The cells that are intact are largely in G1. These data confirm that either Ssd1 or Mpt5 is required, specifically during the postdiauxic and stationary phases of growth, for cell wall modification and achieving a protective, reversible quiescent state.

P-body protein Lsm1 is critical for Q-cell formation and longevity

Yeast cells grown in rich glucose media to stationary phase contain prominent P-bodies (Brengues and Parker, 2007), and Ssd1 associates with these RNA–protein aggregates (Jansen *et al.*, 2009; Kurischko *et al.*, 2011). Using two GFP-tagged components of P-bodies (Dcp2 and Dhh1), we determined that the percentage of cells containing P-bodies was comparable in *SSD1* and *ssd1-d*

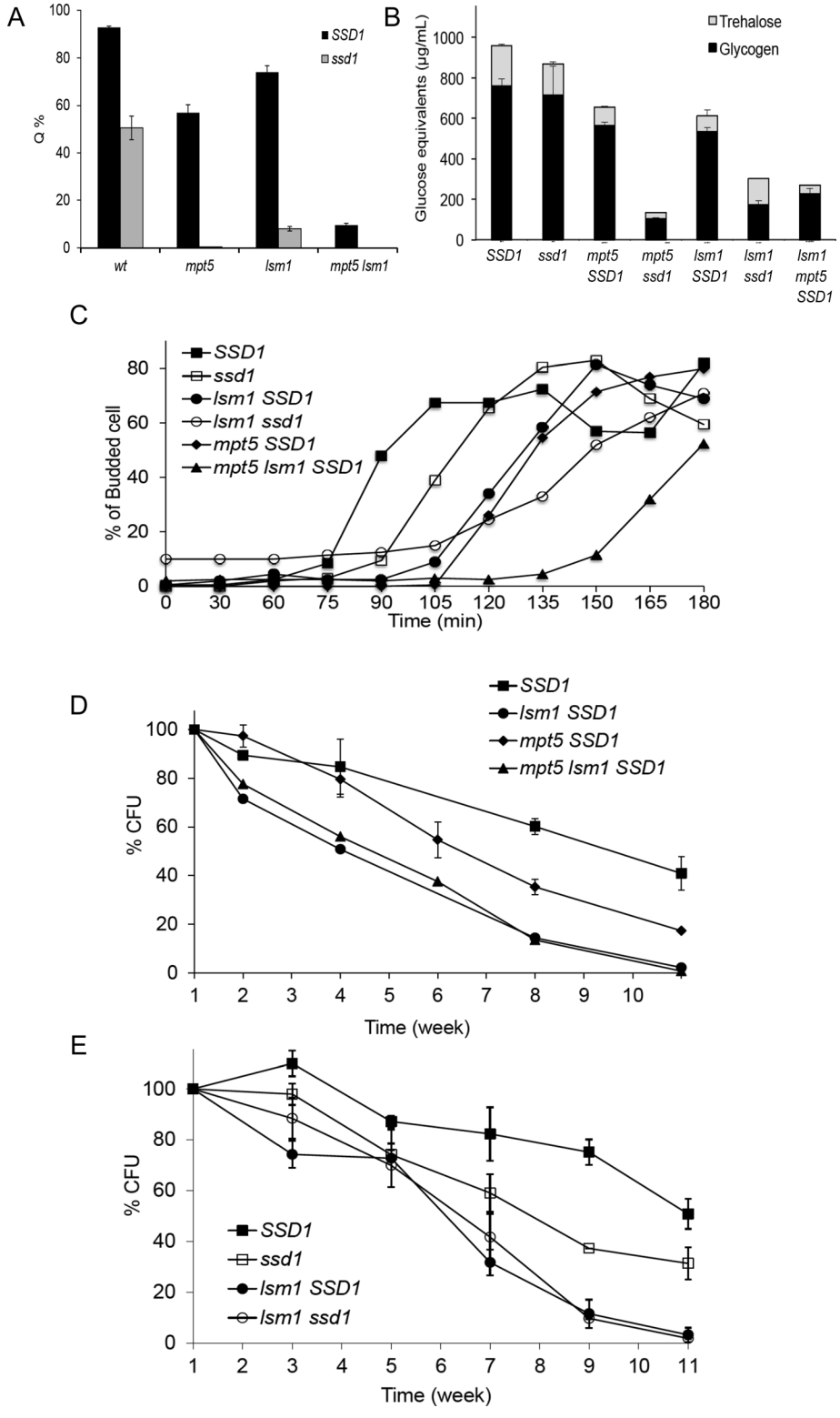

FIGURE 7: Posttranscriptional control is important for Q-cell formation, recovery, and longevity. (A) Yield of Q cells purified from 1-wk-old cultures. (B) Carbohydrate accumulation in stationary-phase cultures after 7 d of growth. (C) Budding kinetics during cell cycle reentry upon refeeding. (D, E) Longevity of Q cells purified from 7-d-old cultures. Genotypes as indicated.

cells (Supplemental Figure S2, A–C). We then asked whether P-body formation was required for the formation or longevity of Q cells using an *edc3* mutant. Edc3 serves as a scaffold for P-body formation but has no effect on mRNA decay or the translational repression that takes place in P-bodies (Decker *et al.*, 2007). As expected, cells carrying this mutation showed no sign of P-body aggregation. Despite lack of P-body aggregates, yield, longevity, and recovery of *edc3* Q cells was identical to those of wild-type W303 *SSD1* cells (Supplementary Figure 2, D–G).

We then eliminated Lsm1, which promotes the decapping and degradation of mRNAs and the translational repression of mRNAs in P-bodies during glucose starvation (Holmes *et al.*, 2004; Coller and Parker, 2005). The single *lsm1* mutant has a modest effect on Q-cell yield (Figure 7A) and carbohydrate accumulation (Figure 7B). The Q cells that are formed are also slower to reenter the cell cycle upon refeeding (Figure 7C). The *lsm1* mutant has little or no effect on the cell wall (Figure 8A) or doubling time or viability in log phase (Figure 8C). It also shows normal G1 arrest and high viability after 7 d of growth (Figure 8D.) However, Lsm1 plays a unique and important role in the longevity of Q cells. The *lsm1SSD1* Q cells have a half-life of 4 wk, compared with 11 wk for *LSM1SSD1*, and there is no further decrease in longevity when either *SSD1* or *MPT5* is also mutated (Figure 7D,E). This is despite the steep decline in Q-cell yield and carbohydrate accumulation in the double mutants (Figure 7, A and B). This suggests that the decapping, translational repression, or some other function of Lsm1, acting downstream of Ssd1 and Mpt5, is important for Q-cell longevity.

The Q cells that can be purified from the double mutants are very delayed in cell cycle reentry when refed, especially *lsm1mpt5*. The *lsm1mpt5* double behaves like wild-type cells (*SSD1*) during log phase (Figure 8C). After 24 h, these cells look normal based on light scattering, but they show no peak of reduced DNA fluorescence (Figure 8A). The *lsm1ssd1-d* cells also show a similar level of DTT-sensitive light scattering but only a small peak of reduced DNA fluorescence. These observations suggest that Mpt5, Ssd1, and Lsm1 contribute specifically to the modification of cell walls during postdiauxic growth. Unlike all the other single and double mutants, the *lsm1ssd1-d* double mutant is defective both early and late in the growth cycle. These cells have a doubling time twice that of *ssd1-d* and show a twofold and threefold drop, respectively, in viability and colony formation during log phase (Figure 8, C and D). We conclude that Ssd1 and Lsm1 have an additional overlapping role in log-phase cells that is not shared by Mpt5.

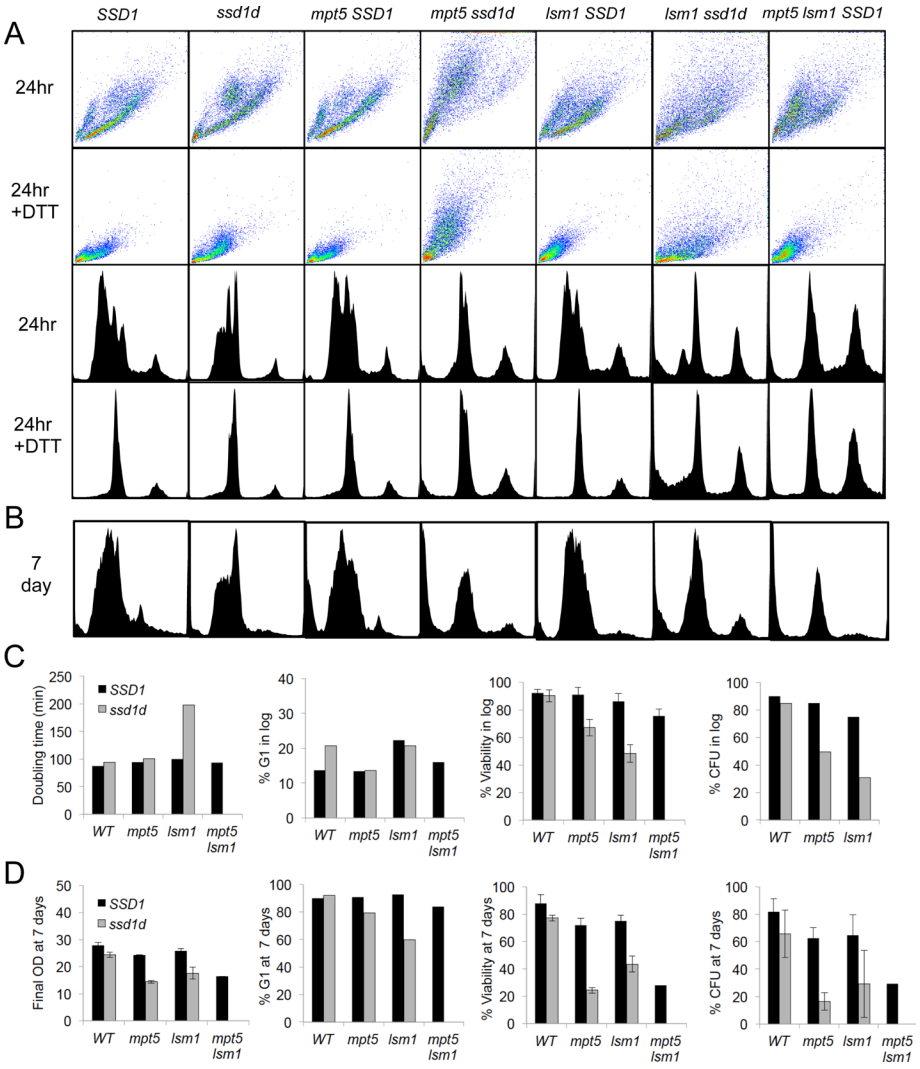

FIGURE 8: Posttranscriptional regulators have stationary-phase-specific functions. (A) Light scattering and DNA fluorescence measurements before and after DTT treatment. (B) DNA fluorescence of 7-d-old cultures. (C) Doubling time, percentage of cells in G1, viability, and colony-forming ability of logarithmically growing cells. (D) Final optical density, percentage of intact cells in G1, viability, and colony-forming ability of cells after 7 f of growth. Genotypes as indicated.

DISCUSSION

In budding yeast, the only known signal to enter quiescence is nutrient limitation. This has led to skepticism that yeast could be an informative model for understanding the mechanisms used to enter, maintain, or exit the quiescent state. It is true that abrupt withdrawal of glucose does not lead to a protective and long-lived population of G1-arrested quiescent cells. It is also true that auxotrophic mutants, which require nutrients (e.g., amino acids) that cells normally make, end up in a nonphysiological starvation state when grown to saturation phase (Henry, 1973; Saldanha *et al.*, 2004; Boer *et al.*, 2008). However, if wild-type, prototrophic yeast are allowed to grow to high density and respond to a diminishing supply of glucose, they are not starved for glucose at all. Instead, they contain much more stored glucose than log-phase cells contain. Moreover, a subset of the cells undergoes a series of changes that differentiate them from the nonQ cells in the population and from rapidly dividing cells. The Q cells that result can be purified from stationary-phase cultures. They are extremely homogeneous, heat tolerant, and uniformly G1 arrested. They display very long life spans in the nondividing state, and upon refeeding they synchronously reenter the cell cycle (Allen *et al.*, 2006; Li *et al.*, 2009).

The events that differentiate Q cells from rapidly dividing cells are initiated before the DS, with a lengthening of G1, as cells adjust to their diminishing glucose supply (Miles *et al.*, 2013). This suggests that cells have evolved a strategy for shifting from a growth mode to a survival mode that is triggered by an early sign of nutrient limitation. They respond by stockpiling their remaining glucose in the form of trehalose and glycogen. These disaccharides and polysaccharides can be used during the arrest and the recovery cycle (Sillje *et al.*, 1999), and they have added benefits as protectants from heat, oxidation, dessication, and salt stress (Elbein *et al.*, 2003). However, our data indicate that strains with equivalent levels of stored carbohydrate can have very different Q-cell yield, thermotolerance, longevity, and cell cycle reentry kinetics, so carbohydrate accumulation is not solely responsible for these quiescent phenotypes.

The cell divisions that take place after the DS give rise to a large population of very small daughter cells. Because daughters predominate in the Q-cell population, we conclude that this asymmetric division contributes to the generation of Q cells as a distinct cellular lineage. Johnston *et al.* (1977) found that prototrophic yeast, limited for nitrogen, arrest in G1 and produce unusually small cells. These small cells were the densest cells in the population, so they could be purified, just as carbon-limited Q cells can be purified. Thus purified, they were used to show that small cells require more time to bud upon refeeding than larger cells. This is consistent with the view that physical growth, in G1, is rate limiting for cell division, but it is complicated by the possibility that these cells may have been coming out of quiescence. These investigators had qualitatively similar findings with sulfur- and phosphate-starved cells, which were later shown to accumulate storage carbohydrates as well (Lillie and Pringle, 1980). We conclude that asymmetric cell division and glucose accumulation are common steps in the log-to-Q transition in response to depletion of at least four basic nutrients.

Q cells contain high levels of stored carbohydrates, but it is not the carbohydrates that pre-Q cells inherit disproportionately. Instead, it is the ability to accumulate and maintain those carbohydrates that is Q cell specific. These Q cells also contain highly functional mitochondria by several measures. Disproportionate inheritance of higher-functioning mitochondria by daughter cells was one of the first cell division asymmetries reported and linked to longevity (Lai *et al.*, 2002; Peraza-Reyes *et al.*, 2010; McFaline-Figueroa *et al.*, 2011). At the transition from proliferation to quiescence, this asymmetry is quite striking and probably determinative. Q cells shift from glycolysis to respiration and maintain

their carbohydrate reserves, whereas nonQ cells continue glycolysis at the expense of those reserves. In this way, nonQ cells resemble cancer cells, which escape quiescence and use glucose to drive proliferation (Warburg, 1956; Vander Heiden *et al.*, 2009).

Cell wall changes are known to take place in stationary-phase cells. Using two flow cytometry assays, we found that these cell wall changes are also initiated early, and they result in Q cells with distinct light scattering profiles that are highly resistant to dye penetration. We found that these two cell wall changes are mechanistically distinct. Both require Sed1 and other disulfide-linked cell wall proteins that can be stripped from cell walls by DTT treatment. The latter requires an overlapping function of Ssd1, Mpt5, and Lsm1 and at least one cell wall protein, Ecm33, whose mRNA is bound by Ssd1 (Hogan *et al.*, 2008; Jansen *et al.*, 2009). Treatment of Q cells with DTT reduces the thermotolerance of these cells, indicating a protective role for the Q-cell wall.

We previously showed that the wild-type *SSD1* allele almost doubles the yield of Q cells in W303 and substantially increases their longevity (Li *et al.*, 2009). The increased Q-cell yield is due to more mother cells entering the Q-cell population. However, they are not as long lived as Q daughters. With our flow cytometry assay, we showed that Ssd1 accelerates the modification of cell walls in mother and daughter cells. The simple interpretation of this is that Ssd1 facilitates Q-cell wall formation by delivering key cell wall mRNAs to P-bodies, where they are stored for later use in cell wall synthesis. This hypothesis is strengthened by the fact that another mRNA-binding protein, Mpt5, also plays a critical, overlapping role with Ssd1 in Q-cell formation. Both *mpt5* and *ssd1-d* single mutants reduce Q-cell yield, and their effects are additive and stationary phase specific. No Q cells are formed in the double mutant.

Mpt5 and Ssd1 interact physically, and both deliver mRNAs to P-bodies. Mpt5 and Ssd1 have been shown to function in parallel to promote cell wall integrity (Kaeberlein and Guarente, 2002) and increase replicative life span, which is the number of cell divisions mother cells can undergo before they die (Kaeberlein *et al.*, 2005). Both Mpt5 and Ssd1 are polymorphic in wild and laboratory strains (Kennedy *et al.*, 1995), which may help explain the variability of Q-cell yield in different genetic backgrounds. P-body aggregation per se is not required for Q-cell formation, but at least one activity residing within P-bodies (Lsm1) is involved.

Lsm1 is critical for the longevity of Q cells. This phenotype is unaffected by defects in either Ssd1 or Mpt5. Ssd1 and Mpt5 play critical redundant roles in Q-cell formation, and they exacerbate the *lsm1* defect in carbohydrate accumulation, cell wall modification, and Q-cell yield. All three proteins are important for the cell cycle reentry of Q cells, and these reentry defects are additive. Our data indicate that Ssd1 binds at least one cell wall mRNA whose product is critical for Q-cell wall modification. We speculate that Mpt5 binds an overlapping or functionally related set of quiescence-specific mRNAs. Both Ssd1 and Mpt5 deliver these mRNAs to P-bodies, where they are protected and then released at the appropriate time. They may interact directly with Lsm1, but our data indicate that other P-body components may also be involved. Mpt5 physically interacts with Dhh1 (Tarassov *et al.*, 2008), and Ssd1 interacts with Pat1 (Kurischko *et al.*, 2011). These proteins, like Lsm1, are important the translational repression of mRNAs during glucose starvation (Holmes *et al.*, 2004; Coller and Parker, 2005). Pat1 and Dhh1 have also been shown to be important for survival in stationary phase (Ramachandran *et al.*, 2011). As such, they are good candidates for acting along with Lsm1 to sequester critical mRNAs that promote a successful transition to quiescence.

In summary, we characterized a series of events that take place as budding yeast transition from a dividing to a nondividing, quiescent state in response to glucose depletion. These cells do not divide until they have exhausted every carbon available to them. Instead, they initiate global shifts in transcription (DeRisi *et al.*, 1997) and translation (Castelli *et al.*, 2011) as glucose becomes limiting. Within hours of scavenging all the glucose in the medium, they undergo highly asymmetric cell divisions and build protective cell walls on the daughters that are destined to become the quiescent population. The resulting Q cells are filled with storage carbohydrates and highly functional mitochondria. They are extremely thermotolerant and long lived. The success of this transition to quiescence critically depends on posttranscriptional regulation directed by Ssd1, Mpt5, and Lsm1.

MATERIALS AND METHODS

Strains and growth conditions

The yeast strains were all derived from W303 (*ssd1-d*). Details are given in Supplemental Table S1. The auxotrophic markers were corrected in all strains, and deletions were made as previously reported (Li *et al.*, 2009). The Abf2-GFP (BY7078), Dhh1-GFP (BY6575, BY6583), and Dcp2-GFP (BY6573, BY6584) with GFP integrated at the C-termini were constructed using pFA6a-GFP (S65T)-Kan as described (Longtine *et al.*, 1998). Reproducible growth curves were obtained by patching cells from fresh plates onto yeast extract/peptone (YEP) plus 2% glycerol and growing them overnight to eliminate petites. This patch was used to inoculate 5 ml of yeast extract/peptone/dextrose (YEPD). Then a further 1/50 dilution was made and grown overnight. This culture was used to inoculate 25 ml of YEPD in a 250-ml flask to an OD_{600} of 0.02 and allowed to grow at 30°C, shaking at 200 rpm. The diauxic shift was defined as the point at which no glucose was detected in the media, which was determined with glucose detection strips (GLU 300; Precision Labs, West Chester, OH). Q cells were purified from YEPD cultures that were 7 d old unless otherwise specified, using a 25-ml Percoll density gradient (Allen *et al.*, 2006) with minor modifications (Li *et al.*, 2009). Q-cell yield is calculated as the percentage of OD_{600} units loaded that sediment to the bottom 9 ml of the gradient. NonQ cells are collected from the top 7 ml of the gradient. Cell viability was assayed by FungaLight and colony-forming units as described (Li *et al.*, 2009). Data plotted were an average from at least two independent experiments. Cell size was measured with a Z2 Beckman Coulter Counter (Beckman Coulter, Brea, CA). Longevity assays were preformed with purified Q cells in water as described (Li *et al.*, 2009). For cell cycle reentry, 10 OD of Q cells were transferred to 20 ml of YEPD medium and aerated at 30°C. Samples were collected every 15 min. Cells were examined microscopically for the presence of new buds. At least 200 cells were examined at each time point.

Cell imaging

Calcofluor and propidium iodide staining. Approximately 10^6 cells were collected and mixed with Calcofluor White M2R (Fluorescent Brightener 28; Sigma-Aldrich, St. Louis, MO) at a final concentration of 100 µg/ml. Cells were incubated at room temperature for 30 min in the dark and then washed twice with 50 mM Tris (pH 7.5). For Figure 5, the cells were then stained with propidium iodide (CAS 25535-16-4; Sigma-Aldrich) at a final concentration of 20 µM for 30 min and washed twice with 50 mM Tris buffer. The cells were examined with a Nikon Eclipse E600 microscope (Nikon, Melville, NY) with a Nikon Plan Apochromat 60×/numerical aperture (NA) 1.40 oil immersion objective and a UV-2E/C

4′,6-diamidino-2-phenylindole filter (excitation at 330–380 nm) for Calcofluor and tetramethylrhodamine isothiocyanate HYQ filter (excitation at 530/550 nm) for propidium iodide. Photographs of cells were taken on a Photometrics Cascade 512B camera with MetaMorph version 6.3r2 software (Molecular Devices, Sunnyvale, CA).

GFP detection. Cells were examined using a Nikon Eclipse E800 microscope with a Nikon 60×/NA 1.40 PlanApo oil immersion objective and a fluorescein isothiocyanate filter (excitation at 460–500 nm). Photographs of cells were taken using a CoolSNAP HQ High Resolution Monochrome CCD Camera (Photometrics, Tucson, AZ) with MetaMorph software.

Phalloidin staining of actin. Approximately 1×10^7 cells were collected and resuspended in 900 µl of phosphate-buffered saline (PBS) buffer (137 mM NaCl, 10 mM phosphate, 2.7 mM KCl, pH 7.4). Cells were then sonicated and fixed with 300 µl of 16% formaldehyde (15710; Electron Microscopy Sciences, Hatfield, PA) for 35 min at 25°C. After washing with PBS, cells were suspended in 200 µl of PBS. A 20-µl amount of 6.6 µM phalloidin (Phalloidin Alex Fluor 546; A22283; Invitrogen, Carlsbad, CA) was added to the solution, and then cells were incubated for 1 h in the dark with rotating. Cells were washed twice with 1 ml of PBS and resuspended in mounting solution containing *p*-phenylenediamine and 90% glycerol. Cells were observed using a DeltaVision RT Wide-field Deconvolution Microscope (Applied Precision, Issaquah, WA) with 100× as objective and rhodamine filter. Images are maximal projection of *z*-stacks performed using a 0.2-µm step. Image acquisition, deconvolution, and analysis were done by using SoftWoRX.

Thermotolerance assay

Purified Q cells, 1 OD_{600}, were spun down and resuspended in 1 ml of water, and cells were incubated between 52 and 55°C for different periods of time as indicated in figure legends and then cooled with ice cold water. The sample tubes were placed on ice until all samples were treated. Then these samples were diluted and plated on YPD plates and incubated for 3 d at 30°C. The percentage of cells able to form colonies was calculated relative to the untreated sample.

Trehalose and glycogen assays

Assays were performed essentially as described (Parrou *et al.*, 1997) and modified (Shi *et al.*, 2010). Culture and Q or nonQ cells, 5 OD_{600}, were processed as described and incubated with amyloglucosidase (10115; Sigma-Aldrich) or trehalase (T8778; Sigma-Aldrich) to convert glycogen or trehalose, respectively, to glucose. Then glucose was assayed in a 96-well platform using a Glucose Assay kit (GAG020; Sigma-Aldrich). Values reported are averages of at least three biological replicates, each with multiple measurements.

Flow cytometry

For flow cytometry, cells were fixed in 70% ethanol for 2 h or overnight, washed once with water, then resuspended in 0.5 ml of 50 mM Tris-HCl (pH 8.0) containing 0.2 mg/ml RNase A and incubated at 37°C for 4 h. These cells were spun down, resuspended in 0.5 ml of 50 mM Tris-HCl (pH 7.5) containing 2 mg/ml proteinase K, and incubated at 50 C for 1 h. They were then spun down again and resuspended in 0.5 ml of 50 mM Tris-HCl (pH 7.5) and stored at 4°C. Before analysis, they were sonicated, pelleted, and resuspended in 0.5 ml of 50 mM Tris-HCl (pH 7.5) with 1.0 µM Sytox Green (Invitrogen). DTT treatment was carried out before ethanol treatment, with 50 mM DTT in 5 mM EDTA, 0.1 M Tris-HCl, pH 8.5, for 15 min at 30°C in all cases except Figure 4I, for which a 30-min DTT treatment was used.

For fluorescence-activated cell sorting (FACS), ~5×10^7 cells were collected from a 24-h culture, and the DNA was stained with Sytox Green as described. Cells were resuspended in 5 ml of 50 mM Tris, pH 7.5, and then gated and sorted in a FACSAria I machine (Becton Dickinson, Franklin Lakes, NJ) with a 70-µm nozzle and a flow rate of 10,000 events/s. Data acquisition and analysis was done with BD FACSDiva Version 6.1.3. Sorted cells were collected in 5-ml tubes in PBS and then spun down in microfuge tubes and stained with Calcofluor White M2R.

ACKNOWLEDGMENTS

We thank D. Gottschling and members of the Breeden lab for useful comments on the manuscript. This work was supported by National Institutes of Health Grant GM41073 (L.B.).

REFERENCES

Allen C *et al.* (2006). Isolation of quiescent and nonquiescent cells from yeast stationary-phase cultures. J Cell Biol 174, 89–100.

Balagopal V, Parker R (2009). Polysomes, P bodies and stress granules: states and fates of eukaryotic mRNAs. Curr Opin Cell Biol 21, 403–408.

Benaroudj N, Lee DH, Goldberg AL (2001). Trehalose accumulation during cellular stress protects cells and cellular proteins from damage by oxygen radicals. J Biol Chem 276, 24261–24267.

Boer VM, Amini S, Botstein D (2008). Influence of genotype and nutrition on survival and metabolism of starving yeast. Proc Natl Acad Sci USA 105, 6930–6935.

Brauer MJ, Huttenhower C, Airoldi EM, Rosenstein R, Matese JC, Gresham D, Boer VM, Troyanskaya OG, Botstein D (2008). Coordination of growth rate, cell cycle, stress response, and metabolic activity in yeast. Mol Biol Cell 19, 352–367.

Brengues M, Parker R (2007). Accumulation of polyadenylated mRNA, Pab1p, eIF4E, and eIF4G with P-bodies in *Saccharomyces cerevisiae*. Mol Biol Cell 18, 2592–2602.

Brengues M, Teixeira D, Parker R (2005). Movement of eukaryotic mRNAs between polysomes and cytoplasmic processing bodies. Science 310, 486–489.

Burtner CR, Murakami CJ, Kennedy BK, Kaeberlein M (2009). A molecular mechanism of chronological aging in yeast. Cell Cycle 8, 1256–1270.

Caron F, Jacq C, Rouviere-Yaniv J (1979). Characterization of a histone-like protein extracted from yeast mitochondria. Proc Natl Acad Sci USA 76, 4265–4269.

Castelli LM *et al.* (2011). Glucose depletion inhibits translation initiation via eIF4A loss and subsequent 48S preinitiation complex accumulation, while the pentose phosphate pathway is coordinately up-regulated. Mol Biol Cell 22, 3379–3393.

Coller J, Parker R (2005). General translational repression by activators of mRNA decapping. Cell 122, 875–886.

Davidson GS *et al.* (2011). The proteomics of quiescent and non-quiescent cell differentiation in yeast stationary-phase cultures. Mol Biol Cell 22, 988–998.

Decker CJ, Teixeira D, Parker R (2007). Edc3p and a glutamine/asparagine-rich domain of Lsm4p function in processing body assembly in *Saccharomyces cerevisiae*. J Cell Biol 179, 437–449.

DeRisi JL, Iyer VR, Brown PO (1997). Exploring the metabolic and genetic control of gene expression on a genomic scale. Science 278, 680–686.

De Virgilio C (2012). The essence of yeast quiescence. FEMS Microbiol Rev 36, 306–339.

De Virgilio C, Hottiger T, Dominguez J, Boller T, Wiemken A (1994). The role of trehalose synthesis for the acquisition of thermotolerance in yeast. I. Genetic evidence that trehalose is a thermoprotectant. Eur J Biochem 219, 179–186.

Elbein AD, Pan YT, Pastuszak I, Carroll D (2003). New insights on trehalose: a multifunctional molecule. Glycobiology 13, 17R–27R.

Elliott B, Futcher B (1993). Stress resistance of yeast cells is largely independent of cell cycle phase. Yeast 9, 33–42.

Francois J, Parrou JL (2001). Reserve carbohydrates metabolism in the yeast *Saccharomyces cerevisiae*. FEMS Microbiol Rev 25, 125–145.

Gadd GM, Chalmers K, Reed RH (1987). The role of trehalose in dehydration resistance of *Saccharomyces cerevisiae*. FEMS Microbiol Lett 48, 249–254.

Hanahan D, Weinberg RA (2000). The hallmarks of cancer. Cell 100, 57–70.
Hanahan D, Weinberg RA (2011). Hallmarks of cancer: the next generation. Cell 144, 646–674.
Henry SA (1973). Death resulting from fatty acid starvation in yeast. J Bacteriol 116, 1293–1303.
Hogan DJ, Riordan DP, Gerber AP, Herschlag D, Brown PO (2008). Diverse RNA-binding proteins interact with functionally related sets of RNAs, suggesting an extensive regulatory system. PLoS Biol 6, e255.
Holmes LE, Campbell SG, De Long SK, Sachs AB, Ashe MP (2004). Loss of translational control in yeast compromised for the major mRNA decay pathway. Mol Cell Biol 24, 2998–3010.
Hottiger T, De Virgilio C, Hall MN, Boller T, Wiemken A (1994). The role of trehalose synthesis for the acquisition of thermotolerance in yeast. II. Physiological concentrations of trehalose increase the thermal stability of proteins in vitro. Eur J Biochem 219, 187–193.
Hoyle NP, Castelli LM, Campbell SG, Holmes LE, Ashe MP (2007). Stress-dependent relocalization of translationally primed mRNPs to cytoplasmic granules that are kinetically and spatially distinct from P-bodies. J Cell Biol 179, 65–74.
Jansen JM, Wanless AG, Seidel CW, Weiss EL (2009). Cbk1 regulation of the RNA-binding protein Ssd1 integrates cell fate with translational control. Curr Biol 19, 2114–2120.
Johnston GC, Ehrhardt CW, Lorincz A, Carter BL (1979). Regulation of cell size in the yeast *Saccharomyces cerevisiae*. J Bacteriol 137, 1–5.
Johnston GC, Pringle JR, Hartwell LH (1977). Coordination of growth with cell division in the yeast *Saccharomyces cerevisiae*. Exp Cell Res 105, 79–98.
Kaeberlein M, Guarente L (2002). *Saccharomyces cerevisiae* MPT5 and SSD1 function in parallel pathways to promote cell wall integrity. Genetics 160, 83–95.
Kaeberlein M, Kirkland KT, Fields S, Kennedy BK (2005). Genes determining yeast replicative life span in a long-lived genetic background. Mech Ageing Dev 126, 491–504.
Kennedy BK, Austriaco NR Jr, Zhang J, Guarente L (1995). Mutation in the silencing gene SIR4 can delay aging in *S. cerevisiae*. Cell 80, 485–496.
Klosinska MM, Crutchfield CA, Bradley PH, Rabinowitz JD, Broach JR (2011). Yeast cells can access distinct quiescent states. Genes Dev 25, 336–349.
Kurischko C, Kim HK, Kuravi VK, Pratzka J, Luca FC (2011). The yeast Cbk1 kinase regulates mRNA localization via the mRNA-binding protein Ssd1. J Cell Biol 192, 583–598.
Lai CY, Jaruga E, Borghouts C, Jazwinski SM (2002). A mutation in the ATP2 gene abrogates the age asymmetry between mother and daughter cells of the yeast *Saccharomyces cerevisiae*. Genetics 162, 73–87.
Laporte D, Lebaudy A, Sahin A, Pinson B, Ceschin J, Daignan-Fornier B, Sagot I (2011). Metabolic status rather than cell cycle signals control quiescence entry and exit. J Cell Biol 192, 949–957.
Li L, Lu Y, Qin LX, Bar-Joseph Z, Werner-Washburne M, Breeden LL (2009). Budding yeast SSD1-V regulates transcript levels of many longevity genes and extends chronological life span in purified quiescent cells. Mol Biol Cell 20, 3851–3864.
Lillie SH, Pringle JR (1980). Reserve carbohydrate metabolism in *Saccharomyces cerevisiae*: responses to nutrient limitation. J Bacteriol 143, 1384–1394.
Longtine MS, McKenzie AIII,, Demarini DJ, Shah NG, Wach A, Brachat A, Philippsen P, Pringle JR (1998). Additional modules for versatile and economical PCR-based gene deletion and modification in *Saccharomyces cerevisiae*. Yeast 14, 953–961.
Lord PG, Wheals AE (1980). Asymmetrical division of *Saccharomyces cerevisiae*. J Bacteriol 142, 808–818.
Lu C, Brauer MJ, Botstein D (2009). Slow growth induces heat-shock resistance in normal and respiratory-deficient yeast. Mol Biol Cell 20, 891–903.
McFaline-Figueroa JR, Vevea J, Swayne TC, Zhou C, Liu C, Leung G, Boldogh IR, Pon LA (2011). Mitochondrial quality control during inheritance is associated with lifespan and mother-daughter age asymmetry in budding yeast. Aging Cell 10, 885–895.
Miles S, Li L, Davison J, Breeden LL (2013). Xbp1 directs global repression of budding yeast transcription during the transition to quiescence and is important for the longevity and reversibility of the quiescent state. PLoS Genet 9, e1003854.
Parker R (2012). RNA degradation in *Saccharomyces cerevisiae*. Genetics 191, 671–702.
Parrou JL, Teste MA, Francois J (1997). Effects of various types of stress on the metabolism of reserve carbohydrates in *Saccharomyces cerevisiae*: genetic evidence for a stress-induced recycling of glycogen and trehalose. 143, 1891–1900.
Peraza-Reyes L, Crider DG, Pon LA (2010). Mitochondrial manoeuvres: latest insights and hypotheses on mitochondrial partitioning during mitosis in *Saccharomyces cerevisiae*. BioEssays 32, 1040–1049.
Pinkston JM, Garigan D, Hansen M, Kenyon C (2006). Mutations that increase the life span of *C. elegans* inhibit tumor growth. Science 313, 971–975.
Ramachandran V, Shah KH, Herman PK (2011). The cAMP-dependent protein kinase signaling pathway is a key regulator of P body foci formation. Mol Cell 43, 973–981.
Ribeiro MJ, Reinders A, Boller T, Wiemken A, De Virgilio C (1997). Trehalose synthesis is important for the acquisition of thermotolerance in *Schizosaccharomyces pombe*. Mol Microbiol 25, 571–581.
Sagot I, Pinson B, Salin B, Daignan-Fornier B (2006). Actin bodies in yeast quiescent cells: an immediately available actin reserve? Mol Biol Cell 17, 4645–4655.
Salazar O, Asenjo JA (2007). Enzymatic lysis of microbial cells. Biotechnol Lett 29, 985–994.
Saldanha AJ, Brauer MJ, Botstein D (2004). Nutritional homeostasis in batch and steady-state culture of yeast. Mol Biol Cell 15, 4089–4104.
Sang L, Coller HA, Roberts JM (2008). Control of the reversibility of cellular quiescence by the transcriptional repressor HES1. Science 321, 1095–1100.
Shimoi H, Kitagaki H, Ohmori H, Iimura Y, Ito K (1998). Sed1p is a major cell wall protein of *Saccharomyces cerevisiae* in the stationary phase and is involved in lytic enzyme resistance. J Bacteriol 180, 3381–3387.
Shi L, Sutter BM, Ye X, Tu BP (2010). trehalose is a key determinant of the quiescent metabolic state that fuels cell cycle progression upon return to growth. Mol Biol Cell 21, 1982–1990.
Sillje HH, Paalman JW, ter Schure EG, Olsthoorn SQ, Verkleij AJ, Boonstra J, Verrips CT (1999). Function of trehalose and glycogen in cell cycle progression and cell viability in *Saccharomyces cerevisiae*. J Bacteriol 181, 396–400.
Talarek N, Cameroni E, Jaquenoud M, Luo X, Bontron S, Lippman S, Devgan G, Snyder M, Broach JR, De Virgilio C (2010). Initiation of the TORC1-regulated G0 program requires Igo1/2, which license specific mRNAs to evade degradation via the 5′-3′ mRNA decay pathway. Mol Cell 38, 345–355.
Tarassov K, Messier V, Landry CR, Radinovic S, Serna Molina MM, Shames I, Malitskaya Y, Vogel J, Bussey H, Michnick SW (2008). An in vivo map of the yeast protein interactome. Science 320, 1465–1470.
Teixeira D, Sheth U, Valencia-Sanchez MA, Brengues M, Parker R (2005). Processing bodies require RNA for assembly and contain nontranslating mRNAs. RNA 11, 371–382.
Tothova Z, Gilliland DG (2007). FoxO transcription factors and stem cell homeostasis: insights from the hematopoietic system. Cell Stem Cell 1, 140–152.
Vander Heiden MG, Cantley LC, Thompson CB (2009). Understanding the Warburg effect: the metabolic requirements of cell proliferation. Science 324, 1029–1033.
Warburg O (1956). On respiratory impairment in cancer cells. Science 124, 269–270.